Int. J. Multiphase Flow Vol. 7, No. 5, pp. 521–543, 1981
Printed in Great Britain.

0301-9322/81/050521-23$02.00/0
Pergamon/Elsevier

THE PREDICTION OF TWO-PHASE MIXTURE LEVEL AND HYDRODYNAMICALLY-CONTROLLED DRYOUT UNDER LOW FLOW CONDITIONS†

K. H. SUN, R. B. DUFFEY and C. M. PENG
Nuclear Safety and Analysis Department, Electric Power Research Institute, 3412 Hillview Avenue, Palo Alto, CA 94304, U.S.A.

(*Received* 13 *February* 1980; *in revised form* 11 *December* 1980)

Abstract—A theory is given for the thermal-hydraulic phenomena during uncovery of a flow channel. This is relevant to a reactor core under typical small break or operational transient conditions. A distinct equivalent collapsed liquid level and a two-phase-mixture level are defined in the model. The former represents the liquid inventory in the channel, while the latter characterizes the heat transfer regimes. The definition of these levels are coupled through the mass and energy conservation equations, and the constitutive relations for void fraction and net vapor generation location.

Analytical solutions are obtained for the transient variation of both the collapsed liquid and the two-phase mixture levels.

The analyses have been compared with existing single-tube data with uniform heat flux, and rod bundle experiments with an axial power profile and inlet feedwater flow. The results demonstrate the potential of the present model for application to reactor conditions.

1. INTRODUCTION

The boiling dry of a flow channel, steam generator tube bundle, a saucepan or a reactor core (NSAC 1979) refers to the situation of gradual depletion of water inventory. The water inventory is often represented by the collapsed liquid level defined by neglecting the vapor bubbles. For the case of very small flow where the acceleration and viscous forces are negligible, the collapsed liquid height is equal to the hydrostatic head of water. To define the heat transfer conditions during the uncovery of a core, a relevant parameter is the level of the two-phase mixture. The height of the two-phase mixture is generally marked as a discontinuity in the axial void distribution and in the surface temperature. The two-phase level therefore represents the limit of the hydrodynamically controlled dryout point for the heated surface, which is only wet and in nucleate boiling below that level. This dryout process is therefore also termed "uncovery," as the two-phase mixture evaporates.

To evaluate the void fraction below the two-phase mixture level, it is necessary to determine three thermal-hydraulic parameters. These are (1) the location of the net vapor generation, z_{NVG}, at which vapor bubbles begin to form and collapse while the bulk temperature is subcooled, (2) the location where the bulk fluid reaches the saturation temperature, z_{sat}, and (3) the equilibrium level, z_{eq}, at which the net vapor flow equals to the inlet water flow and above which the liquid flow rate is zero (see figure 1a). In practice, the equilibrium level is the lowest level of uncovery for a given inlet flow and subcooling. Evaluation of these three parameters, together with the void fraction, allows the prediction of the two-phase mixture height.

The paper utilizes the already available correlations for void fraction in two-phase flow, in which the vapor and liquid have unequal velocities. The key assumptions which enable direct solution lie in the recognition of the quasi-steady nature of the flow, and that the major heat release occurs only below the two-phase mixture level. This two-phase level represents a heat transfer and hydrodynamic discontinuity. The theory is applied to boiling channels with an axial power profile and subcooled inlet flow including considerations of the effects of the inlet flow being via a vertical down-comer, and of the reflux condensation of the vapor. A simple

†Presented at the 19*th Natl Heat Transfer Conf.*, Orlando, Florida, 27–30 July, 1980.

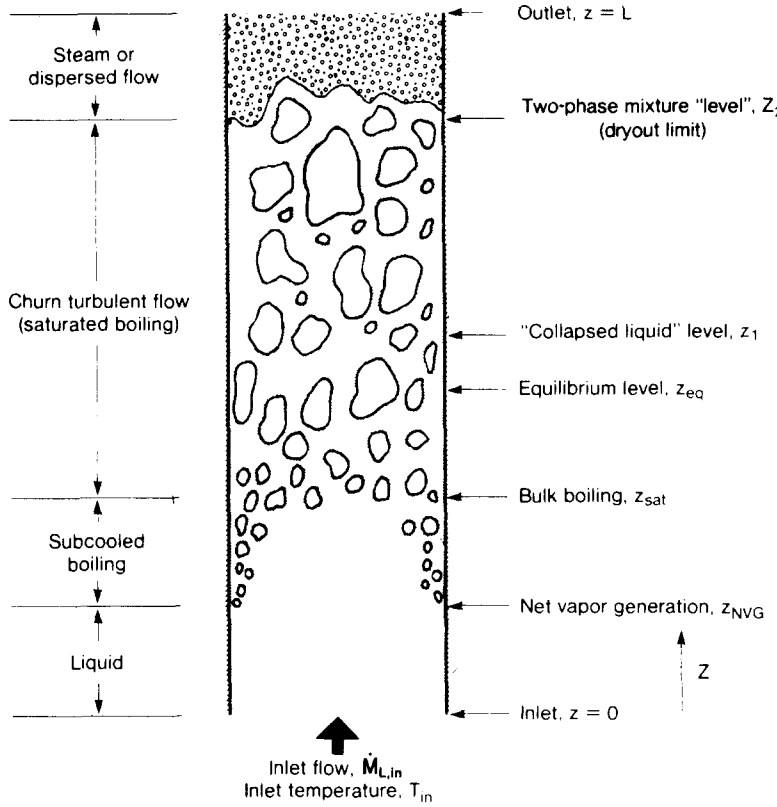

Figure 1(a). Schematic diagram of a vertical flow channel uncovering or boiling dry due to a wall heat flux.

closed-form solution is derived for the case of axially uniform power with zero inlet flow. Comparisons are presented to data obtained in tubes and pin bundles over a wide range of flows and ambient pressures.

2. TWO-PHASE LEVEL THEORY

2.1 *Physical model*

The physical system under consideration is a vertical flow channel, either heated by the peripheral walls, or by powered rods inside the channel as in a reactor core. The heat flux from the walls may be axially uniform, or may vary in a cosine profile. Only a low feedwater flow enters the channel, and hence the channel is in a "boiling dry" condition, the liquid gradually evaporating at a rate strongly dependent on the wall heat flux. For the general case where liquid enters the channel with flow rate, $\dot{M}_L$, and temperature, T_{in}, the typical thermal-hydraulic conditions in the channel are as illustrated in figure 1(a).

The subcooled liquid is heated as it flows upward. As the temperature reaches saturation, vapor bubbles start forming at a location called the "net vapor generation" level, z_{NVG}. Below z_{NVG} the fluid is single-phase liquid whereas above, subcooled boiling exists to an elevation, z_{sat}, where the bulk fluid reaches the saturation temperature. Above z_{sat}, saturated boiling occurs until the two-phase mixture level, z_2, is reached.

The flow regime in these boiling regions varies from bubbly flow to churn-turbulent flow as the void fraction increases. However, above the two-phase mixture level, the flow regime is generally dispersed droplet flow or single-phase steam. Associated with these flow conditions, the two relevant levels (in addition to z_2, z_{sat} and z_{NVG}) are the collapsed liquid level, z_1, and the equilibrium level, z_{eq}. Here, the fictitious height, z_1, characterizes the liquid inventory and is conveniently defined and easily measured. Also, z_{eq} is the height at which the vapor flow rate equals the inlet liquid flow and hence represents the minimum level of channel uncovery.

It is noted that the thermal hydraulic conditions described above are similar to a reflooding case (Seban *et al.* 1978). The major difference lies in the balance of the power input and the cooling capacity of the inlet feedwater. In the reflooding case, the cooling water drives a rewetting front which progresses upward removing the stored energy: whilst in the uncovery case, the power input boils the liquid away to cause a dryout front which recedes downward.

2.2 *Approximations and assumptions*

We wish to determine the two-phase level and liquid inventory in a boiling channel or pin bundle. In order to provide an analytical solution, we analyze the flow utilizing a one-dimensional equilibrium model with an algebraic interphase velocity relationship. The basic approximation is that the transient two-phase level behavior is sufficiently slow that a quasi-steady analysis is appropriate. Hence, incompressibility of the phases is assumed since sonic wave propagation effects are negligible, flashing is negligible for slow pressure transients, and saturation temperature conditions are assumed for the two-phase mixture above the net vapor generation region. The adequacy of these approximations will be tested by comparison to data. Since we need to track the two-phase level, we utilize the Beringer–Zuber drift-flux model commonly used for analysis of boiling flows (Zuber & Staub 1966, 1967, Ward 1979, Wallis 1969). The results are presented in analytical form to high-light the physics of the flow. The effects of subcooled inlet flow and subcooled boiling are incorporated utilizing conventional correlations.

Typical total system flow paths are illustrated schematically in figure 1(b). The steam flow is vented, and for some cases a fraction, ϵ, may be condensed and returned to the downcomer, together with any injected water.

The present analysis differs from that considered for "pool swell" numerical analysis as discussed by Vea & Lahey (1978) and Ward (1978), which allowed for decompression effects in tracking the two-phase mixture. The present analysis does yield a closed form analytical solution, and shows clearly the physical phenomena relevant to slow transients; i.e. the heat transfer is strongly coupled to the flow regimes and phase separation. The model also differs from that of Wedekind, Bhatt & Beck (1979) who assumed a time-invariant average void fraction for the whole tube upstream of the two-phase mixture level. Their result is shown later in section 4 to be a special limiting case of the present model.

2.3 *Conservation laws*

We proceed by considering a one-dimensional boiling flow with the liquid and vapor flowing at unequal velocities. In conventional notation, the flux of phase, k, at elevation z, is defined as:

$$j = \sum_k j_k \quad \text{and} \quad j_k = \alpha_k u_k \qquad [1]$$

where $\alpha_k = \alpha_k(z)$ is the volume fraction of phase k, which are the liquid, L, and vapor, G, for the present case.

We consider cross-sectional averages across the flow channel. The instantaneous mixture density is as usual,

$$\rho_m = \sum_k \alpha_k \rho_k = \rho_L(1-\alpha) + \rho_G \alpha \qquad [2]$$

where $\alpha \triangleq \alpha_G$. We define a "collapsed liquid height", z_1, such that from mass conservation,

$$\int_{z_{NVG}}^{z_1} \rho_L \, dz = \int_{z_{NVG}}^{z_2} \rho_m \, dz . \qquad [3]$$

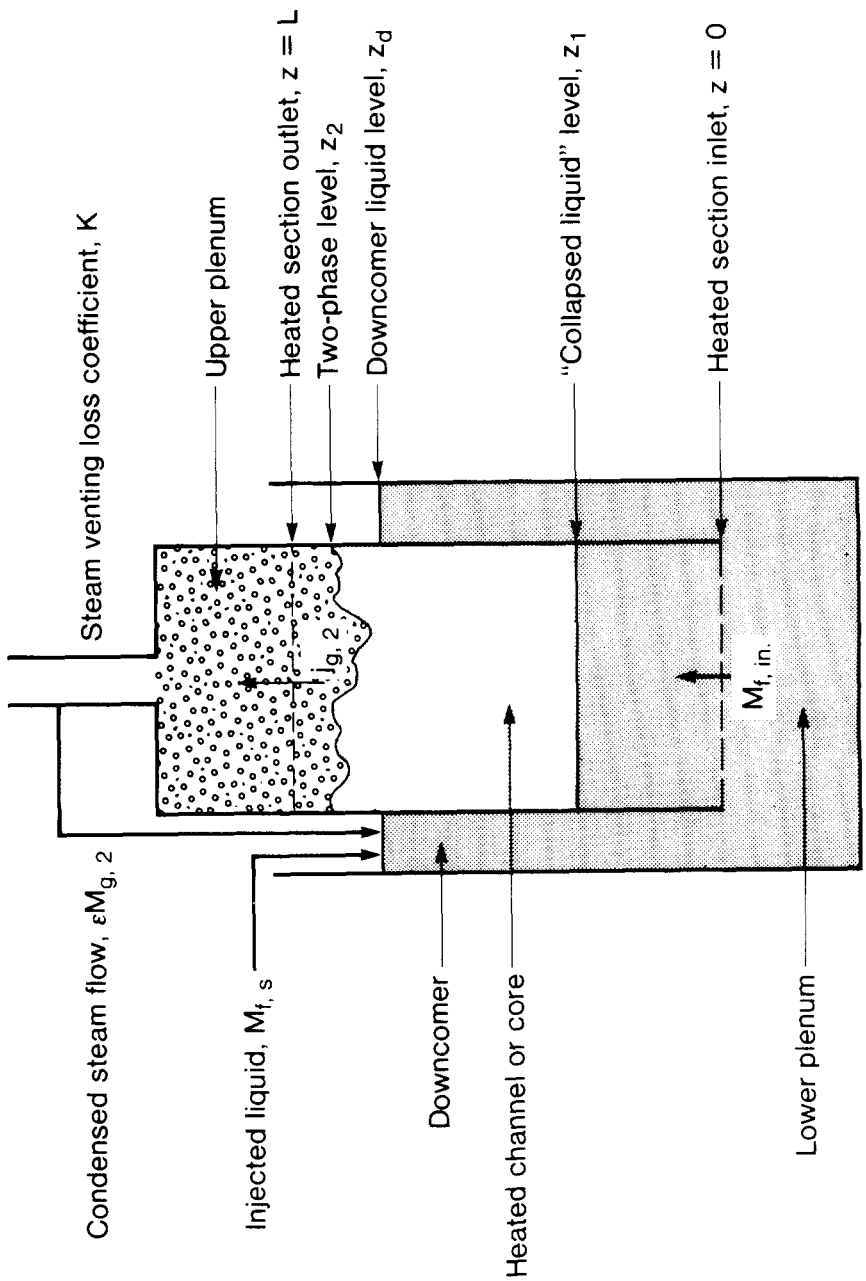

Figure 1(b). Schematic of system flows during uncovery with a downcomer feed and partial condensation of venting steam.

Here z_{NVG} represents the elevation of net vapor generation since the inlet liquid may be subcooled. For a saturated inlet flow, of course, $z_{NVG} \simeq 0$, since both wall and liquid superheats are small. Note that z_1 is a fictitious height which represents the liquid inventory in the two-phase region.

Hence z_2 is the height of the two-phase mixture, which is usually a sharp discontinuity in void fraction, with

$$\alpha \simeq 1 \quad \text{for } z \geqslant z_2.$$

Physically this marks the transition from bubbly or churn-turbulent flow to high quality mist or pure vapor flow. From [2] and [3] we obtain

$$z_1 - z_{NVG} = \int_{z_{NVG}}^{z_2} \left(1 - \alpha + \alpha \frac{\rho_G}{\rho_L}\right) dz \qquad [4]$$

The void fraction below the two-phase mixture level must be characterized by a void fraction correlation of either drift flux (Zuber *et al.* 1965, 1966, 1967), or empirical correlation forms (Wilson *et al.* 1962, Cunningham & Yeh 1973), respectively.

In the drift flux formulation, the vapor drift velocity V_{Gj}—the rate of which vapor separates from the two-phase mixture—is defined as

$$V_{Gj} = u_G - C_0 j = \frac{j_G}{\alpha} - C_0 j \qquad [5]$$

where the distribution parameter, C_0, corrects the void profile for non-uniform radial effects so that:

$$C_0 = \langle \alpha j \rangle / \langle \alpha \rangle \langle j \rangle$$

and

$$V_{Gj} = \langle \alpha V_{Gj} \rangle / \langle \alpha \rangle$$

where $\langle\ \rangle$ represents the usual cross-sectional averaging operator. Recasting [5], the void fraction relation is

$$\alpha = \frac{j_G}{C_0 j + V_{Gj}}. \qquad [6.1]$$

The alternative formulation utilizes an empirical correlation developed by Wilson *et al.* (1962) which can be expressed as

$$\alpha = C_1 \left(\frac{\rho_G}{\rho_L - \rho_G}\right)^{C_2} \left(\frac{j_G}{j}\right)^{0.6} \mathrm{Ku}^{C_3} \left(\frac{\sigma}{D_e^2 g(\rho_L - \rho_G)}\right)^{C_4/2} \qquad [6.2]$$

where $C_1 = 0.564$, $C_2 = 0.12$, $C_3 = 0.67$, $C_4 = 0.1$ for $0 < \mathrm{Ku} < 1.5$, and $C_1 = 0.619$, $C_2 = 0.12$, $C_3 = 0.47$, $C_4 = 0.1$ for $1.5 < \mathrm{Ku} < 10$. Ku is the non-dimensional steam velocity defined by

$$\mathrm{Ku} = j_G / \{\sigma g(\rho_L - \rho_G)/\rho_L^2\}^{0.25}. \qquad [6.3]$$

Ku is often called the Katateladze number. In the present calculation, we also utilize the

empirical correlation developed by Cunningham & Yeh (1973) which is in the form:

$$\alpha = C_1\left(\frac{\rho_G}{\rho_L}\right)^{C_2}(\mathrm{Ku})^{C_3}\left(\frac{j_G}{j}\right)^{C_4} \qquad [6.4]$$

where $C_1 = 0.70$, $C_2 = 0.24$, $C_3 = 0.67$, and $C_4 = 0.60$ for $\mathrm{Ku} < 1.53$ and $C_1 = 0.76$, $C_2 = 0.24$, $C_3 = 0.47$, and $C_4 = 0.60$ for $\mathrm{Ku} \geq 1.53$.

The vapor and liquid continuity equations are, respectively,

$$\frac{\partial}{\partial t}(\alpha\rho_G) + \frac{\partial}{\partial z}(\alpha\rho_G u_G) = \Gamma \qquad [7.1]$$

$$\frac{\partial}{\partial t}[(1-\alpha)\rho_L] + \frac{\partial}{\partial z}[(1-\alpha)\rho_L u_L] = -\Gamma \qquad [7.2]$$

where Γ is the vapor generation rate per unit volume.

Assuming steady incompressible flow and integrating [7] over the two-phase and collapsed liquid regions, respectively, we obtain

$$j_{G,2} = \frac{1}{\rho_G}\int_0^{z_2} \Gamma \, \mathrm{d}z \qquad [8.1]$$

$$j_{L,1} - j_{L,\mathrm{in}} = \frac{-1}{\rho_L}\int_0^{z_2} \Gamma \, \mathrm{d}z \qquad [8.2]$$

where the temporal changes are assumed small compared to the spatial variations, i.e. $\mathrm{d}\alpha/\mathrm{d}t \ll \mathrm{d}j/\mathrm{d}z$ which is applicable for slow transients, and we neglect the small terms due to the two-phase interface motion. For the downcomer we obtain the mass balance as,

$$\frac{\mathrm{d}z_d}{\mathrm{d}t} = \frac{\dot{M}_{L,s}}{\rho_L a_d} + \frac{a_c}{a_d}\left[\epsilon j_{G,2}\frac{\rho_G}{\rho_L} - V_{L,\mathrm{in}}\right] \qquad [8.3]$$

where ϵ is the fraction at the outlet steam flow that is condensed and returned to the downcomer, $M_{L,s}$ is the system flow injected into the downcomer, and $V_{L,\mathrm{in}}$, is the flow entering the heated channel.

The rate of vaporization flow at the mixture level z_2 is equivalent to the rate of depletion of the liquid inventory allowing for the recondensed flow. This relation can be obtained from [8.1] and [8.2] and can be expressed by,

$$\frac{\mathrm{d}z_1}{\mathrm{d}t} = -j_{G,2}\rho_G/\rho_L + V_{L,\mathrm{in}} \qquad [9]$$

where $\mathrm{d}z_1/\mathrm{d}t$ is simply the liquid flux $j_{L,1}$ at the collapsed liquid height.

2.4 *Loop momentum equations*

The momentum equation is required for cases when the inlet flow velocity, $V_{L,\mathrm{in}}$ is not specified but depends on the system geometry and flow paths (see figure 2). For the low flow velocities of interest here, gravitational forces dominate the pressure losses in the downcomer and heated section. The loss incurred by venting and condensing the steam through pipework and heat exchangers can be treated by a lumped outlet loss coefficient, K_{out}, and that due to the water flowing through the inlet by K_{in}. Consistent with our quasisteady approximations we can

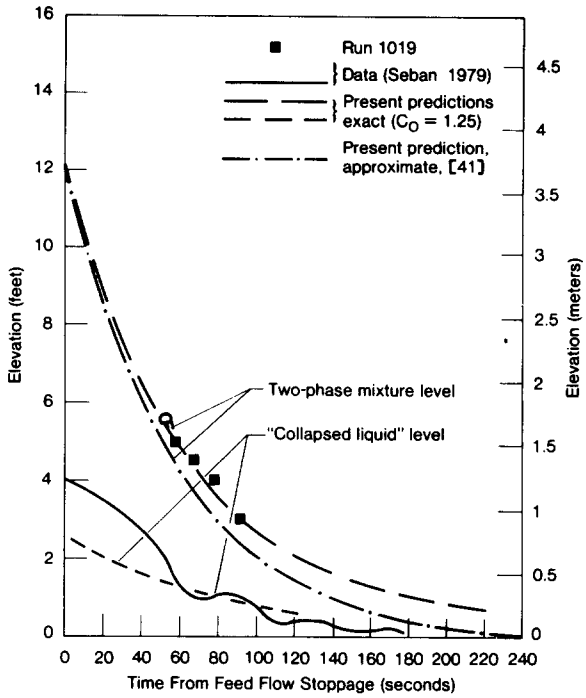

Figure 2. Comparison of exact and approximate analysis with single tube data.

neglect the acceleration and inertial terms, so that the loop momentum equation is simply,

$$\rho_L g(z_d - z_1) = K_{\text{out}} \frac{\rho_G j_{G,2}^2}{2} + K_{\text{in}} \frac{\rho_L V_{L,\text{in}}^2}{2}. \qquad [10]$$

Combining [10] with the mass conservation [8.3] and [9], we obtain the result for the inlet flow velocity as,

$$\frac{K_{\text{in}} V_{L,\text{in}}}{g} \frac{\mathrm{d}V_{L,\text{in}}}{\mathrm{d}t} + \left(1 + \frac{a_c}{a_d}\right) V_{L,\text{in}}$$

$$= \frac{\dot{M}_{L,s}}{\rho_L a_d} + \frac{\rho_G j_{G,2}}{\rho_L} \left[\frac{a_c}{a_d} \epsilon + 1 - \frac{K_{\text{out}}}{g} \frac{\mathrm{d}j_{G,2}}{\mathrm{d}t}\right]. \qquad [11]$$

The loop geometry is now coupled to the channel inlet flow conditions; for many practical cases with low flows we find $z_d \simeq z_1$ and momentum effects may be negligible.

2.5 *Energy equations*

From the mixture energy equation for saturated boiling, the vapor is generated by the wall heat flux only, so

$$\int_0^z \Gamma \, \mathrm{d}z = \frac{\int_0^z q'' p \, \mathrm{d}z - \dot{M}_{L,\text{in}} C_{pL}(T_{\text{sat}} - T_{\text{in}})}{a_c h_{LG}} \qquad [12.1]$$

or, combining with [8.1] we obtain

$$j_G = \frac{\int_0^z q'' p \, \mathrm{d}z - \dot{M}_{L,\text{in}} C_{pL}(T_{\text{sat}} - T_{\text{in}})}{\rho_G h_{LG} a_c} \qquad [12.2]$$

where $q'' = q''(z)$ due to the axial power profile. In deriving [12.1] the assumption has been made that the flashing term is small compared to the vaporization due to the heat flux, i.e.

$$\alpha_k \frac{Dh_k}{Dt} \ll \frac{q''}{\rho_k D_e}$$

which is valid for the slow depressurizations ("quasi-steady") of interest.

The problem of interest is to predict the liquid inventory in the channel, which is characterized by the collapsed liquid level, z_1, and also the heat transfer interface, which is represented by the two-phase mixture level, z_2. To arrive at a solution, it is necessary to relate the mass and energy equations, [7], [8], and [12], to z_1 and z_2. From [12.2], z_2 is related to the vaporization rate at z_2 by

$$j_{G,2} = \frac{\int_0^{z_2} q'' p \, dz - \dot{M}_{L,in} C_{pL}(T_{sat} - T_{in})}{\rho_G h_{LG} a_c} \qquad [12.3]$$

The location z_{sat} where the inlet water flow reaches the saturation temperature can be easily calculated from the obvious energy balance relation,

$$\int_0^{z_{sat}} q''(z) p \, dz = C_{pL} \dot{M}_{L,in}(T_{sat} - T_{in}). \qquad [13]$$

The equilibrium two-phase level, z_{eq}, is defined as the level at which the vapor flow rate is equal to the inlet water flow rate and above which there is no gross upward water flow. Similar to [13], z_{eq} can be easily calculated by

$$\int_0^{z_{eq}} q''(z) p \, dz = \dot{M}_{L,in}[C_{pL}(T_{sat} - T_{in}) + h_{LG}]. \qquad [14]$$

The equilibrium level represents the asymptotic ($t \to \infty$) state for the channel. It should be noted that now we have five simultaneous equations, [4], [6], [9], [11] and [12.3] for the solution of the unknowns, $V_{L,in}$, z_1, z_2, α, and $j_{G,2}$. Ultimately, the solutions provide z_1 and z_2 as a function of time during the channel uncovery process.

3. CONSTITUTIVE RELATIONS

We need the appropriate constitutive models for z_{NVG} and α for the various flow regimes (subcooled nucleate, saturated nucleate and churn-turbulent boiling flows). We adopt the philosophy of taking existing well-established correlations from the literature. In principle, other functional forms may be adopted as necessary. It is not our approach here to adjust the correlations for our case.

Essentially, this relates to the choice of relations for C_0 and V_{G_j}, the drift parameters specified in [6.1], the various constants in [6.2], and z_{NVG} as described in [3]. We wish to use simple conventional formulations. It is known that in this simple representation, C_0 is a function of pressure and also of void fraction. Correlations of the Bankoff—Jones form then have the dependency,

$$C_0 = C_0(P/P_c, \alpha)$$

where P/P_c is the reduced pressure.

For V_{G_j} the conventional single-bubble representation of bubbly and churn-turbulent flow are taken. More complex formulations can be adopted as necessary, but the overall physics is

unaltered. One example is the turbulent void fraction model of Ardron & Hall (1979). The specific forms for the void fraction correlations used in the present study are discussed in sections 3.2 and 3.3 on subcooled and saturated boiling.

3.1 *Treatment of subcooled boiling*

The location of net vapor generation, z_{NVG}, can be calculated by the correlation of Saha & Zuber (1974). For a Peclet number,

$$\mathrm{Pe} = \frac{\rho_L V_L D_h C_{pL}}{k_L}, \leqslant 7 \times 10^4 \qquad [15]$$

$$\mathrm{Nu} = \frac{q'' D_h}{k_L (T_{sat} - T_\lambda)} = 455. \qquad [16]$$

The fluid temperature, T_λ, at z_{NVG}, can be deduced from the simple energy balance relation:

$$T_\lambda = T_{in} + \int_0^{z_{NVG}} q''(z) p \, dz / \dot{M}_L C_{pL}. \qquad [17]$$

For $\mathrm{Pe} \gg 7 \times 10^4$,

$$\mathrm{St} = \frac{q''}{\rho_L V_L C_{pL} (T_{sat} - T_\lambda)} = 0.0065. \qquad [18]$$

It should be noted that since q'' in [16] and [18] is the local heat flux, to obtain z_{NVG} from [17] requires iterations between [16] and [17] or [17] and [18] depending on the range of the Peclet number.

3.2 *Void fraction for the subcooled region*

To calculate the void fraction in the region between z_{NVG} and z_{sat} (the subcooled region), the drift flux expression, [6], can be rearranged for convenience in terms of the local quality, i.e.

$$\alpha = \frac{X}{C_0[X + (1 - X)\rho_G/\rho_L] + V_{G_j}\rho_G/\rho_L V_{L,in}}. \qquad [19]$$

The distribution parameter, C_0, can be obtained from the correlation developed by Dix (1971) for the case of low flow forced convection subcooled boiling; i.e.

$$C_0 = \beta \left[1 + \left(\frac{1}{\beta} - 1\right)^d\right] \qquad [20]$$

where

$$\beta = \frac{X}{X + (1 - X)\rho_G/\rho_L} \qquad [21]$$

and

$$d = (\rho_G/\rho_L)^{0.1} \qquad [22]$$

and V_{G_j} is appropriate for turbulent *bubbly* flow

$$V_{G_j} = 1.18 \left(\frac{\sigma g(\rho_L - \rho_G)}{\rho_L^2}\right)^{1/4} (1 - X(z)). \qquad [23]$$

The quality X can be calculated using the approach of Saha & Zuber (1974), that is a profile fit of the form

$$X = \frac{X_{eq} - X_{NVG} \exp(X_{eq}/X_{NVG} - 1)}{1 - X_{NVG} \exp(X_{eq}/X_{NVG} - 1)} \quad [24]$$

where X_{NVG}, the equilibrium equality at the location of net vapor generation is given by

$$X_{NVG} = -0.0022 q'' D_h C_{pL}/k_L h_{LG} \quad \text{for} \quad Pe \leq 7 \times 10^4 \quad [25]$$

and

$$X_{NVG} = -154 q''/\rho_L h_{LG} V_{L,in}, \quad \text{for} \quad Pe > 7 \times 10^4. \quad [26]$$

The equilibrium thermodynamic quality can be simply obtained from the energy balance relation for any elevation

$$X_{eq} = \int_0^z q'' p \, dz/\dot{M}_{L,in} h_{LG} - C_{pL}(T_{sat} - T_{in})/h_{LG}. \quad [27]$$

3.3 *Void fraction for the saturated region*

The saturated region starts from the saturated elevation, z_{sat}, to the two-phase mixture level, z_2. The inlet feedwater becomes saturated at z_{sat} and continues to boil off above z_{sat} until it reaches the equilibrium level, z_{eq}, above which there is no gross upward water flow. To calculate the void fraction for this region, either the drift flux relation, [19], or the empirical relation, [6.2], is used.

For the value of C_0, we take the form proposed by Jones (1961) and empirically modified by Lellouche (1974) and Lellouche & Zolotar (1979) to fit a wide range of boiling data, i.e.

$$C_0 = \frac{1}{0.82 + 0.18 P/P_c} \quad [28]$$

for tubes and rod bundles. For low pressure conditions, C_0 is about 1.2.

For the drift velocity, we take the Zuber & Findlay (1965) expression for churn-turbulent flow,

$$V_{G_j} = 1.41 \left[\frac{\sigma g(\rho_L - \rho_G)}{\rho_L^2}\right]^{1/4}. \quad [29]$$

The alternative formulation of [6.2] has the pressure and geometry dependencies incorporated in the correlation groups. We taken the two forms which are available in the literature. These are based on data from pipes (Wilson *et al.* 1962) and rod bundles (Cunningham & Yeh 1973), the latter absorbing the geometric dependency into the constant C_1.

Comparisons with rod bundle data (Ardron *et al.* 1977) show that the empirical void fraction correlations, [6.2], are generally superior to the simpler drift models, [6.1], particularly in the pressure and geometric dependencies.

3.4 *Heat flux profile*

A correct description of the heat flux profile is a necessary input for the calculation of core uncovery rate. For slow transient conditions where the change of the stored energy in the wall and the axial conduction near the two-phase mixture level can be neglected, the wall heat flux

below z_2 equals the rate of power generation in the wall and goes into boiling water. For a uniform power profile, [8] and [12] can be easily integrated to show that the vapor flow rate is proportional to the distance from bottom of the flow channel.

For reactor applications, a chopped cosine profile is prevalent. The algebraic superposition form commonly adopted is

$$q''(z) = q_0'' + (\hat{q}'' - q_0'') \cos\left[\frac{\pi}{L}\left(z - \frac{1}{2}\right)\right]$$

where L is the equivalent length of the heated section, and q_0'' and $\hat{q}''$ are the base and the peak of the power profile, respectively. When the profiles are given, [8] and [12] can be integrated straightforwardly to yield j_G and j_L. However, iterations are needed to use [16] or [18] for the calculation of z_{NVG}.

4. METHODS OF SOLUTION

4.1 *General numerical solutions*

For the nonuniform power case with a finite subcooled inlet flow, we must solve the full nonlinear simulataneous equations [4], [6], [9], [12.3] and [17] for the unknowns z_{NVG}, z_1, z_2; α and $j_{G,2}$. The appropriate constitutive relations for $V_{G_j}(\alpha, z)$ and C_0 are given by [19]–[29]. An iterative procedure is again adopted, given the inlet boundary conditions $\dot{M}_{L,in}$ and T_{in} and the system pressure, P. For the cases where the system pressure losses are important, the additional unknown inlet flow, $V_{L,in}$, is obtained by simultaneous solution of [11]. This numerical procedure is incorporated into the computer code UNCOVER whhich has been used for the comparisons given below.

4.2 *Solution for channel uncovery with constant heat flux and no inlet feedwater*

The system under consideration is a vertical circular flow channel with constant wall heat flux. Initially, saturated water filled or reflooded the channel up to a certain level. The level is allowed to decrease by stopping the inlet feedwater flow. For this case, [4], [6.1], [9] and [12.3], can be reduced to the following simple forms:

$$\frac{dz_1}{dt} = \frac{\dot{Q}z_2}{\rho_L h_{LG} a_c} \quad [30]$$

$$j_G = \frac{\dot{Q}z}{\rho_G h_{LG} a_c} \quad [31]$$

$$z_1 = \int_0^{z_2} (1 - \alpha)\, dz \quad [32]$$

and

$$\alpha = \frac{j_G}{C_0 j_G + V_{G_j}} \quad [33]$$

where we have taken $\rho_G/\rho_L \ll 1$ in forming [31] and [32], and $\dot{Q}$ is the total power generation per unit length.

From [30] to [33], we note that there are four unknowns, j_G, α, z_1 and z_2, to be solved.

To obtain a solution for z_1 and z_2, it is necessary first to eliminate the parameters j_G and α. This can be achieved by combining [31] and [33] to obtain an expression for α as a function of the elevation, z, and then to insert the resulting expression into [32]. Integration then leads to the following relation between z_1 and z_2:

$$z_1 = \left(\frac{C_0 - 1}{C_0}\right)\left[z_2 + \frac{\rho_G h_{LG} a_c V_{G_j}}{C_0(C_0 - 1)\dot{Q}} \ln\left(1 + \frac{z_2 C_0 \dot{Q}}{\rho_G h_{LG} V_{G_j} a_c}\right)\right]. \quad [34]$$

By taking a derivative of [34] with respect to time, [34] and [30] can be combined to eliminate z_1 and to lead to the following expression for z_2:

$$-\frac{\dot{Q}z_2}{\rho_L h_{LG} a_c} = \left[\left(\frac{C_0-1}{C_0}\right) + \frac{1}{C_0}\frac{V_{G_j}\rho_G h_{LG} a_c}{\dot{Q}C_0 z_2 + V_{G_j}\rho_G h_{LG} a_c}\right]\frac{dz_2}{dt}. \quad [35]$$

For practical interest,

$$\frac{\dot{Q}C_0 z_2}{V_{G_j}\rho_G h_{LG} a_c} \gg 1. \quad [36]$$

Equations [34] and [35] can be reduced to

$$z_1 = \left(\frac{C_0-1}{C_0}\right)\left[z_2 + \frac{\rho_G h_{LG} a_c V_{G_j}}{C_0(C_0-1)\dot{Q}} \ln \frac{z_2 C_0 \dot{Q}}{\rho_G h_{LG} V_{G_j} a_c}\right] \quad [37]$$

and

$$-\frac{\dot{Q}z_2}{\rho_L h_{LG} a_c} = \left[\frac{C_0-1}{C_0} + \frac{V_{G_j}\rho_G h_{LG} a_c}{\dot{Q}C_0^2 z_2}\right]\frac{dz_2}{dt}. \quad [38]$$

Further simplifications can be made for the cases where

$$(C_0-1) \gg \frac{V_{G_j}\rho_G h_{LG} a_c}{\dot{Q}C_0 z_2}. \quad [39]$$

This reduces [38] to the simple explicit form:

$$\frac{dz_2}{dt} = -\left(\frac{C_0}{C_0-1}\right)\frac{\dot{Q}}{\rho_L h_{LG} a_c} z_2. \quad [40]$$

With the initial condition, $z_2(0) = z_{20}$ where z_{20} is the initial two-phase mixture level, the solution for [40] is

$$z_2(t) = z_{20} \exp\left[-\left(\frac{C_0}{C_0-1}\right)\frac{\dot{Q}}{\rho_L h_{LG} a_c} t\right]. \quad [41]$$

Once $z_2(t)$ is obtained from [41], $z_1(t)$ can be calculated from [37]. The solution for z_1 and z_2 illustrate the relative importance of the various parameters, particularly the sensitivity to the radial distribution coefficient C_0 of the Drift Flux correlation (Zuber & Findley 1965). It is shown that for a given system of geometry, fluid and inventory, the governing parameters for the uncovery transient are the power generation $\dot{Q}$ and the distribution coefficient C_0.

From [32] and [41] we can see that

$$\frac{z_2}{z_1} = \frac{1}{(1-\bar{\alpha})} \simeq \frac{C_0}{C_0-1} \quad [42]$$

where $\bar{\alpha}$ is the average axial void fraction ($\sim 1/C_0$). Hence, the above solution, [41], is equivalent to that given by Wedekind *et al.* (1978) who used the assumption that the system mean void fraction, $\bar{\alpha}$, was time invariant. Their equilibrium model is therefore a special limiting case of the general solution of the present governing equations subject also to the restraint given by [36] and [39].

When the input flow is via a downcomer, and subject to the above approximations, we find the level varies as,

$$z_2(t) = z_{20} \exp\left[-\frac{C_0\dot{Q}}{(C_0-1)\rho_L h_{LG} a_c(1+a_d/a_c)}\, t\right] \qquad [43]$$

where the exit losses are assumed to be small. Therefore, the effect of the downcomer is only to change the effective liquid inventory and time constant by the term $(1 + a_d/a_c)$.

5. COMPARISON OF THEORY WITH EXPERIMENTS

5.1 *Experiments*

To evaluate the theory systematically, we compare with successively more complicated and exacting experiments, i.e.

(1) Simple single tube data with uniform, constant power, which examine the essential physics of the theory and benchmarks the analysis.

(2) Multi-pin bundle data with nonuniform power in which the inlet conditions are known, but a more complex and relevant geometry is introduced.

(3) Transient system data with time varying boundary conditions, which now provides confidence in the theory for application purposes.

The essential features of the experiments are given in Table 1.

5.2 *Comparisons with single tube data*

These experiments consisted of quenching a preheated 3.66-m (12-ft) long vertical tube using cold water, and then stopping the inlet flow (Seban *et al.* 1978, Seban 1979) while maintaining a constant input power. The tube therefore boiled dry, and measurements were made of the total differential pressure (equivalent to the "collapsed" level, z_1) and the wall temperatures.

In figure 2(a) typical comparison is shown with both the analytic solution, [41], and the complete numerical solution of the full differential equation [30] and [34] with C_0 and V_{Gj} calculated from [28] and [29]. The agreement between experiment and analysis is encouraging. Some secondary flow or level transients can be seen in the data, which are at least partly attributable to the transient nature of the experiments. The analytic approximation is quite accurate, except at very long times when dz_2/dt is small.

5.3 *Comparison with rod bundle data*

We first examine experiments in which a bundle of 161-heaters was filled with water and then boiled dry (Wong & Hochreiter 1979). The axial position where the surface temperature increased sharply was taken at the location of the two-phase level. In figure 3(a)–(c), we compare

Table 1.

Experiment	Type	Power	Pressure	Facility	Reference
1.	Single Tube	Uniform	10^5 N/m^2	UC-B/EPRI Berkeley, Ca.	Seban 1979
2.1	161 Rod Bundle	Nonuniform	1.4-4.10^5 N/m^2	FLECHT-SEASET Pittsburgh, Pa.	Hochreiter 1979
2.2	9 Rod Bundle	Uniform	10^5 N/m^2	EPRI/SUNYAB, Buffalo, N.Y.	Chon 1980
3.1	25 Rod bundle	Nonuniform	6x10^6 N/m^2	NRC Semiscale INEL, Idaho	Shumway 1979
3.2	5x10^4 Rod	Nonuniform	6x10^6 N/m^2	GPU TMI-2 reactor, Pa.	NSAC 1979

the present theory with these data for three available pressures. Except for the long times, the data are contained between the limits of the three correlation forms ([6.1], [6.2], [6.4]). The drift formulation sensitivity to the choice of C_0 is shown in figure 3(d), the larger values causing a smaller void fraction ($\sim 1/C_0$) and hence a longer boil-off time.

The agreement is improved somewhat by adopting a value of $C_0 \sim 1.25$, which is less than the largest value obtained at low flows (Nicklin *et al.* 1962). A more exacting test is with the measured void profiles (figure 4a–c). The empirical correlations fit the data at the lower elevations, but are uncertain for the upper portions of the bundle. At higher pressures, the differences become much less (figures 3e and 4d) because of the increased vapor density. The variation of the calculated steam velocity, $j_{G,2}$, as shown in figures 5a–c for the three pressures, is sensitive to the void fraction profiles below the two-phase mixture level.

Other experiments with a 9-heater bundle, but with uniform power, have also been carried out (Chon 1980). The comparisons are shown in figure 6 and the agreement for z_2 is within 20 per cent as for the larger bundle experiments, although there is an underprediction of the collapsed liquid height in this case.

5.4 *Comparison with system data*

A series of experiments have been run on a heated loop simulating a PWR small break and core uncovery sequence (Larson *et al.* 1979). The loop contained a 4-m long 25-rod bundle. In the test designated TMI-3I, at a high system pressure (~60 MN/m^2) the bundle was allowed to

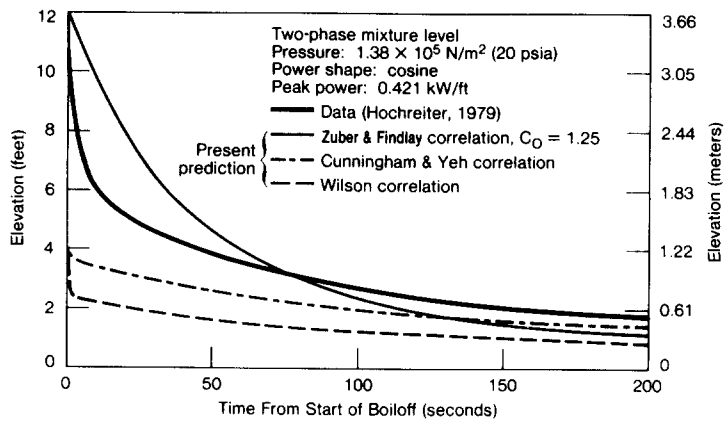

Figure 3(a). Comparison of present model with 161-rod bundle data at 20 psia with no inlet flow.

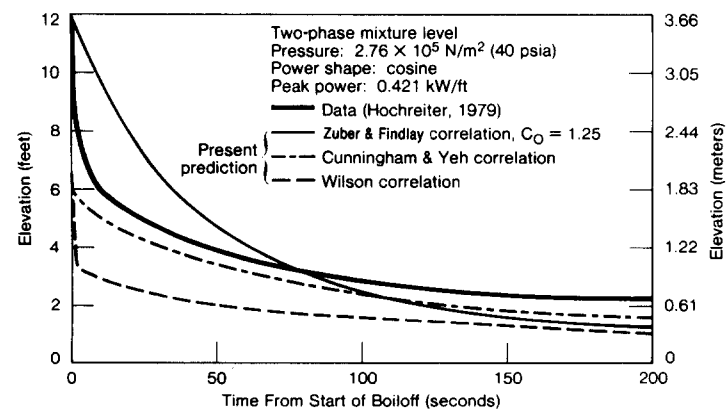

Figure 3(b). Comparison of present model with 161-rod bundle data at 40 psia with no inlet flow.

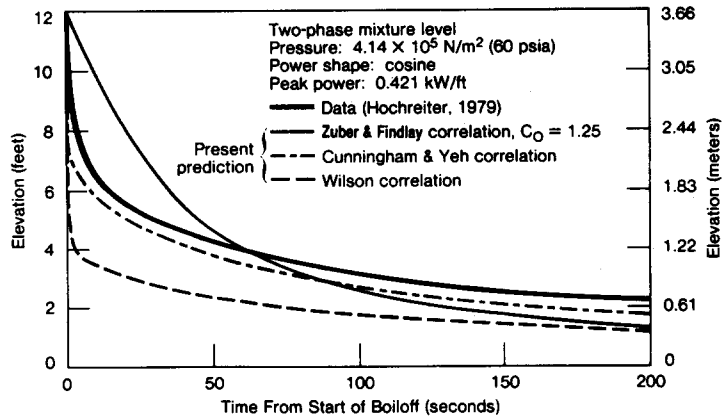

Figure 3(c). Comparison of present model with 161-rod bundle data at 60 psia with no inlet flow.

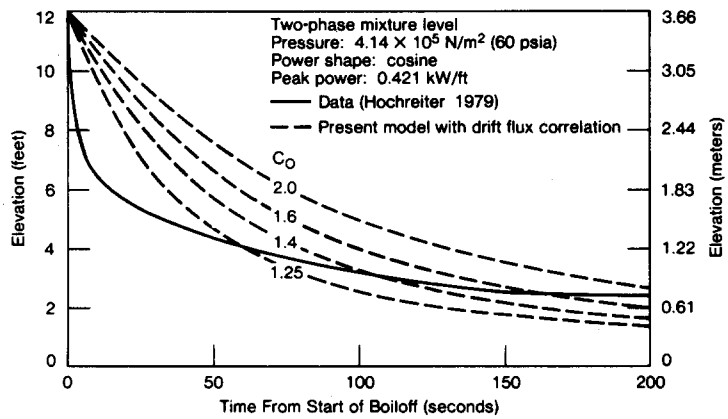

Figure 3(d). Comparison with 161-rod bundle data—sensitivity to the drift flux correlation distribution parameter C_0.

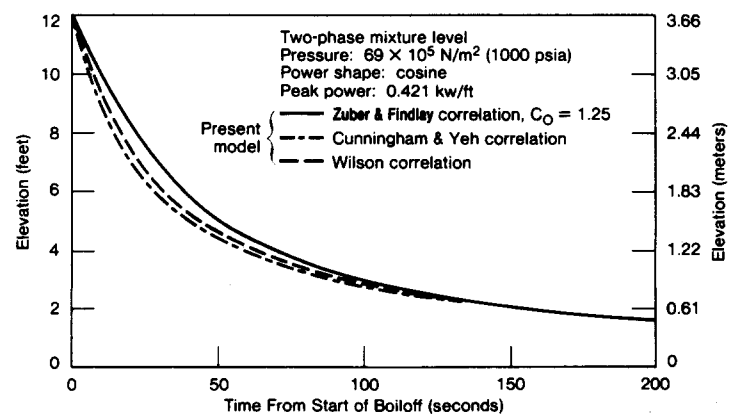

Figure 3(e). Calculated two-phase level vs time for 161-rod bundle at 1000 psia showing sensitivities of various void fraction correlations.

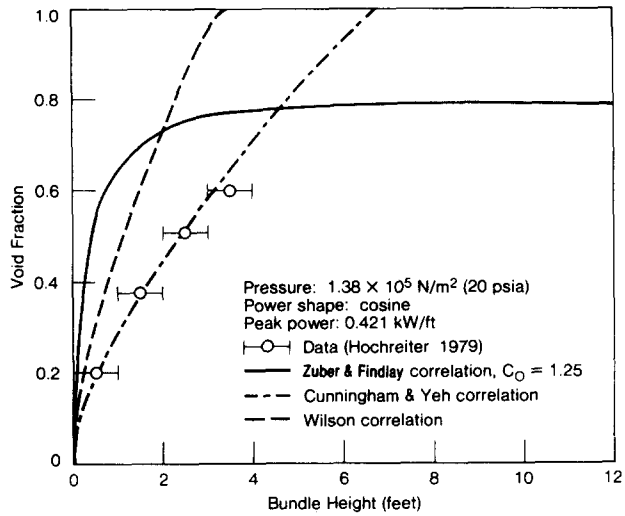

Figure 4(a). Comparison of various void fraction correlations with 161-rod bundle test data at 20 psia with no inlet flow.

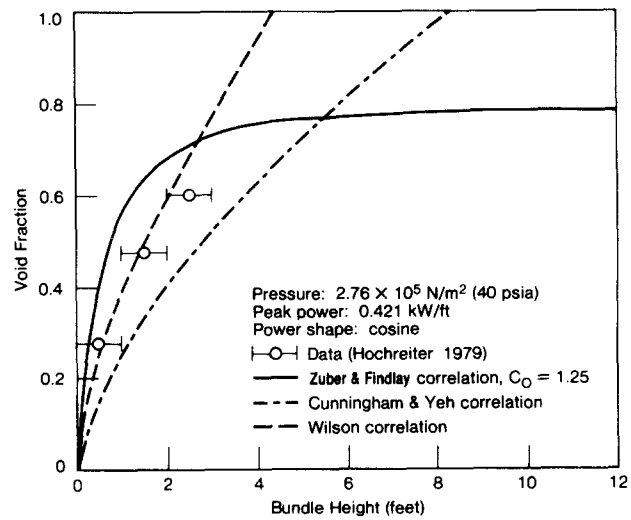

Figure 4(b). Comparison of various void fraction correlations with 161-rod bundle data at 40 psia with no inlet flow.

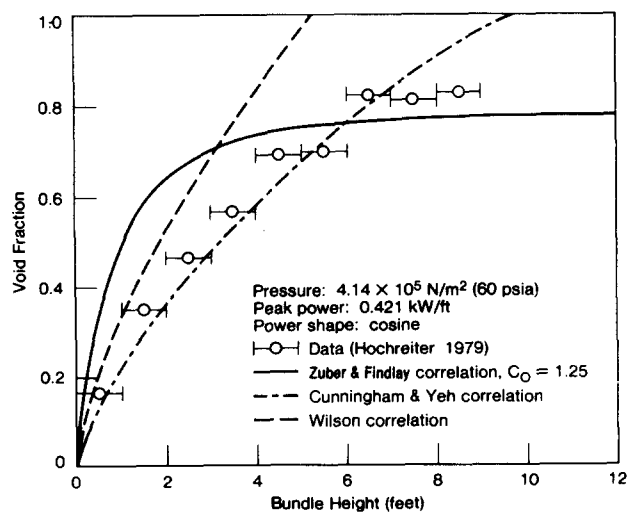

Figure 4(c). Comparison of various void fraction correlations with 161-rod bundle data at 60 psia with no inlet flow.

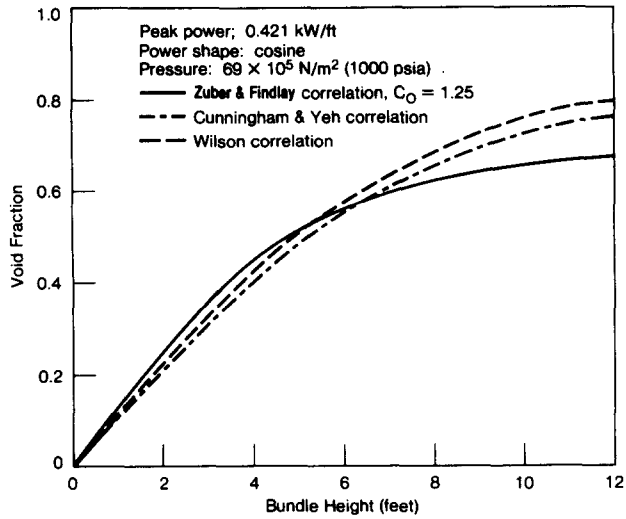

Figure 4(d). Calculated void fraction profiles for the 161-rod bundle at 1000 psia.

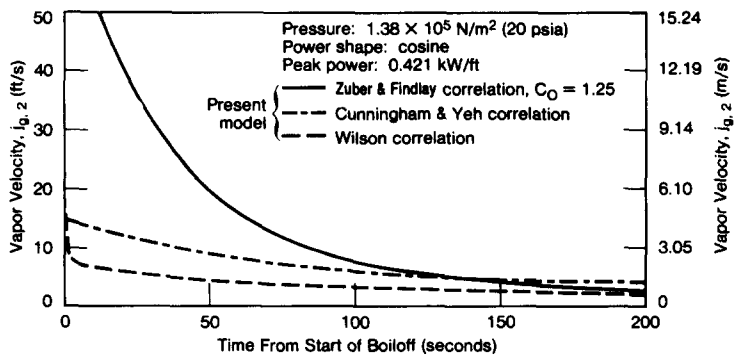

Figure 5(a). Calculated bundle exit vapor velocity vs time for the 161-rod bundle at 20 psia with no feed flow.

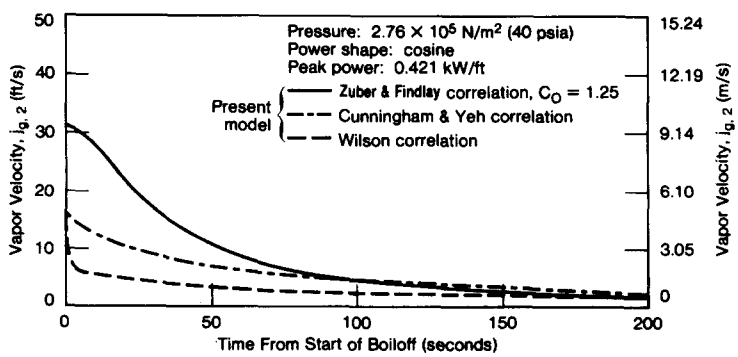

Figure 5(b). Calculated bundle exit vapor velocity vs time for the 161-rod bundle at 40 psia with no inlet flow.

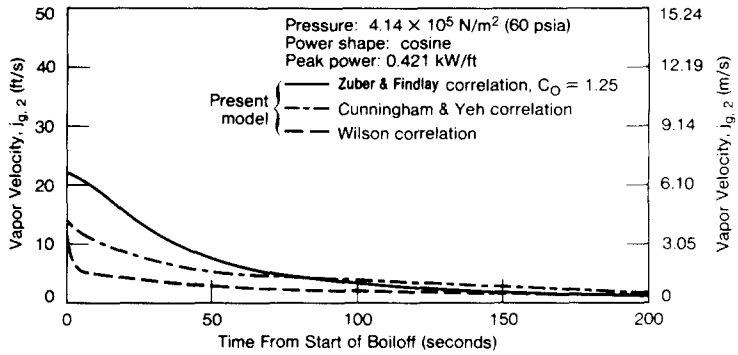

Figure 5(c). Calculated bundle exit vapor velocity vs time for the 161-rod bundle at 60 psia with no feed flow.

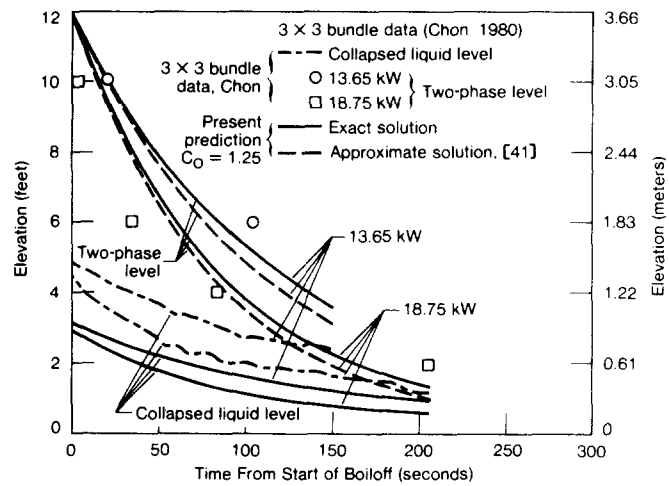

Figure 6. Comparison of 3 × 3 bundle data with the present predictions.

dry out, measurements of the levels z_1 and z_2 being made by densitometry and differential pressure. For the present analysis, the bundle boundary conditions are required. Although the bundle inlet flow is highly uncertain, estimates have been made on the basis of system mass balances and the available flow instrumentation (Shumway 1979). Utilizing the best estimates for the transient flow, the comparison is shown in figure 7(a). We see immediately a systematic underprediction; however, this is within the flow uncertainty which is of order of a factor of two. The sensitivity to the inlet flow is illustrated in figure 7(b): this is not proportional because of the cosine axial power profile.

The general trends are reclaimed, and this is encouraging because of the complexity not only of the experimental transient but also of the system geometry and boundary conditions (*cf.* the single tube experiments).

The final experiment is the reactor accident sequence at the TMI-2 plant, an 880 MW(e) two-loop PWR. Some 6×10^3 s into the transient the reactor cooling systems and pumps were stopped, leading to core uncovery. An analysis of this case utilizing the available plant data has been presented elsewhere (NSAC 1979). Utilizing the known pressure and power conditions and the estimated core flow, the present analysis gives the result shown in figures 8(a)–(c). The rods are not completely uncovered due to the continued small flow to the core, and the result is relatively insensitive to the exact form of the void fraction relation. The agreement between the present theory and the inferred data is encouraging. Figure 8(b) is a composite of all available

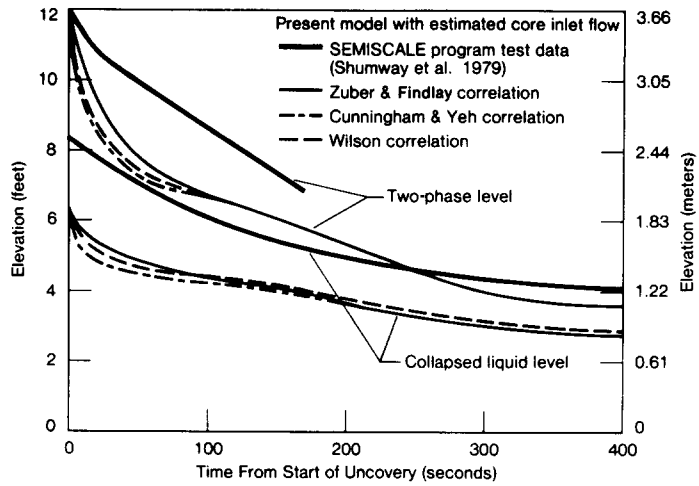

Figure 7(a). Comparison of present model with SEMISCALE small break core uncovery test data showing the sensitivity of various void fraction correlations.

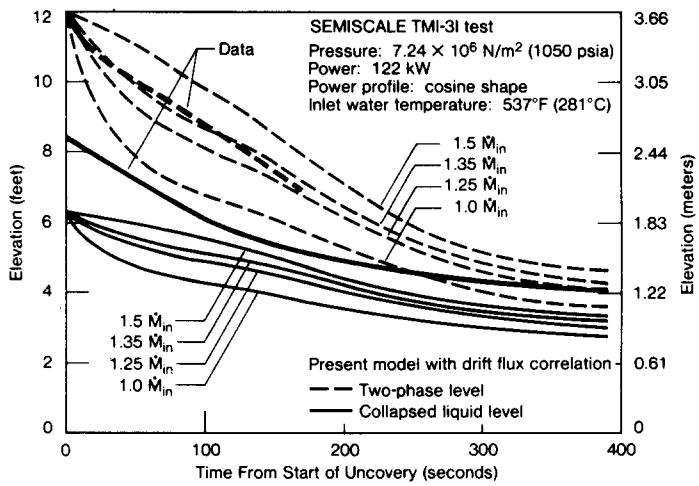

Figure 7(b). Comparison of present model with SEMISCALE small break core uncovery test data.

analyses: shown is the result obtained utilizing the nodal code RELAP-4 (Behling 1979), which clearly overpredicts the core uncovery rate; the prediction assuming no voidage (Cole 1979) which overpredicts the inventory and hence underpredicts the uncovery rate; the results from the nonequilibrium nodal code TRAC (Ireland *et al.*, 1980); and the revised estimates for the reactor (NSAC 1980).

The vapor velocity (figure 8c), shows a transition from the initial state to the new equilibrium value evaporating the inlet water. The vapor velocities imply a mixed free and forced convective laminar flow above the two-phase level.

The above comparisons show that all existing dryout data can be predicted within the experimental uncertainties in flow and the limits of the available void fraction correlations, the uncertainties in flow dominating at the higher pressures. In all results to date, the region of subcooled boiling is a small (<5 per cent) fraction of the two-phase height, indicating that the void generated in the subcooled boiling region might be neglected for practical calculations of the two-phase mixture levels.

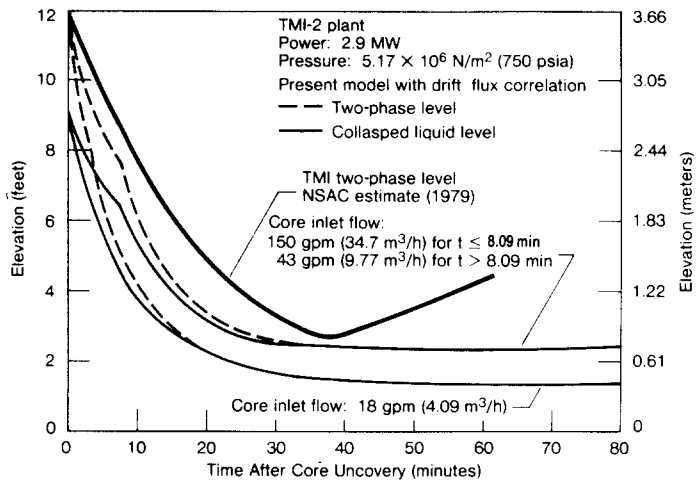

Figure 8(a). Core uncovery vs time for the TMI-2 plant accident for various estimates of the core inlet flow.

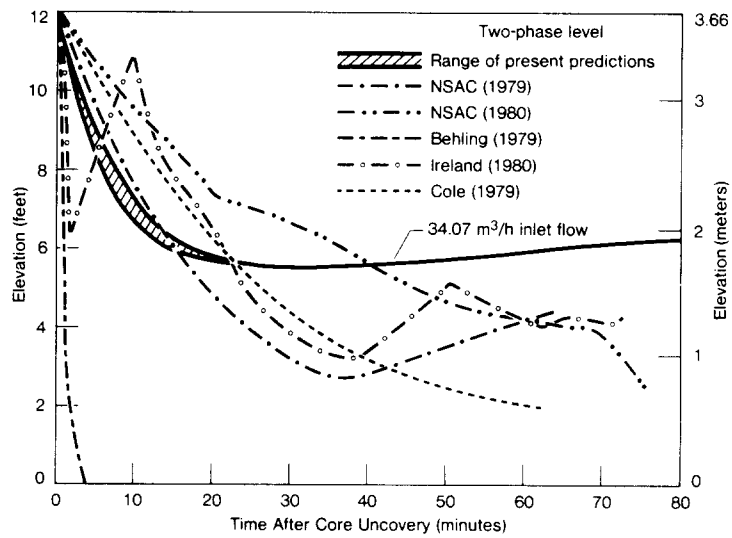

Figure 8(b). Core uncovery for the TMI-2 plant accident with various models.

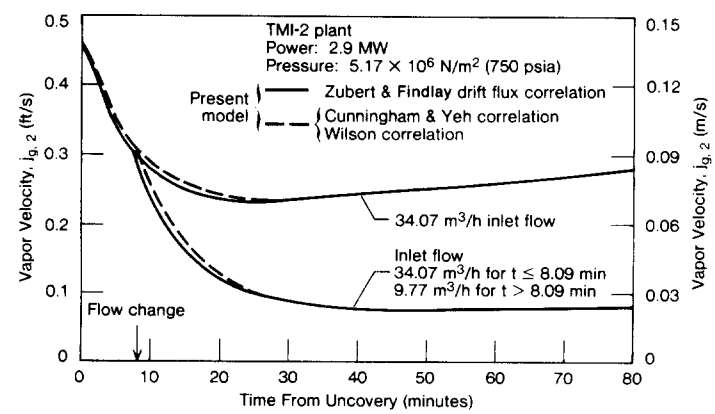

Figure 8(c). Core exit vapor velocity vs time for the TMI-2 plant accident following core uncovery for various estimates of the core inlet flow.

6. CONCLUSIONS

A phenomenologically based thermal-hydraulic model has been developed for the prediction of the rate of uncovery of a flow channel or a reactor core under typical small break or operational transient conditions. The two-phase level marks the hydrodynamically-controlled dryout elevation as the channel boils dry.

The rate of decrease of the collapsed liquid level and the two-phase mixture level has been shown to be sensitive to the distribution parameter in the void fraction correlation at low pressures where the vapor density is small compared to the liquid density. The low vapor density results in vapor velocities generally much higher than the vapor separation or drift velocity. At higher pressures, the results are relatively insensitive to the exact form of the void fraction correlations utilized in the present analysis because of the increased vapor density and decreased voidage.

For the typical uncovery conditions, the rate of uncovery has been shown to be one to three orders of magnitude lower than the drift velocity. This justifies the quasi-steady assumptions used in the analysis.

The agreement between the present analytical predictions and experimental data from the available single-tube and rod bundle data is generally within the experimental uncertainties. This has demonstrated the applicability of the model for reactor conditions. This also shows that the momentum equation is only important for determining the loop flow rates for slow transients, and not the channel thermal conditions. The vapor mass flow rate at the two-phase level has been computed, and can be used as a boundary condition for the post-dryout analysis above the dryout elevation.

NOMENCLATURE

a	flow area
C_p	specific heat
C_0	distribution parameter
D_e	equivalent diameter
D_h	hydraulic diameter
g	gravitational acceleration
h	enthalpy
h_{LG}	latent heat of vaporization
j	superficial volumetric flux
k	thermal conductivity
K	loss coefficient
Ku	Kutateladze number, defined in [6.3]
$\dot{M}$	mass flow rate
Nu	Nusselt number
$\dot{Q}$	heat generation per unit length
q''	heat flux per unit area
P, P_c	pressure and critical pressure
Pe	Peclet number
p	heated perimeter
St	Stanton number
T, T_{in}	temperature and inlet temperature
T_λ	liquid temperature at net vapor generation
t	time
$V_L, V_{L,in}$	liquid velocity and inlet velocity
V_{Gj}	drift velocity
u	velocity
X	quality

z elevation from base of channel
α void fraction
ρ density
Γ volumetric vapor generation rate
σ surface tension

Subscripts

c channel
d downcomer
k pertaining to phase k
m two-phase mixture
L liquid
G vapor
s system
1 equivalent liquid
2 two-phase
NVG net vapor generation
eq equilibrium condition
sat saturation condition
in inlet
0 initial value
out outlet

Acknowledgement—The authors wish to express their gratitude to Mr. C. Lin for his assistance in completing the calculations and to Drs. G. S. Lellouche, J. Kim and G. Srikantiah for their helpful comments.

REFERENCES

ARDRON, K. H. & HALL, P. C. 1978 Prediction of void fraction in low velocity vertical bubbling flows. CEGB Rep. RD/B/N3966 (presented at *European Two-Phase Flow Group Meeting*, Stockholm, Sweden, 29 May–1 June 1978).

ARDRON, K. H., DUFFEY, R. B. & HALL, P. C. 1977 Studies of the physical models used in transient two-phase flow analysis. *Proc. I. Mech. Engng Conf., Heat and Fluid Flow in Water Reactor Safety*, October, Manchester, U.K., pp. 89–96.

BEHLING, S. R. 1979 RELAP4 application to TMI-2 accident. Paper presented at *USNRC 7th Water Reactor Safety Research Information Meeting*, November, Gaithersburg, Maryland.

CHON, W. Y. 1980 Private communication.

COLLIER, J. G. 1972 *Convective Boiling and Condensation*. McGraw-Hill, New York.

COLE, R. K. 1979 Generation of hydrogen during the first three hours of the Three-Mile Island Accident. NRC Rep. NUREG/CR-0912 (Sandia Laboratories).

CUNNINGHAM, J. P. & YEH, H. C. 1973 Experiments and void correlation for PWR small-break LOCA conditions. *Trans. Am. Nucl. Soc.* **17**, 269.

DIX, G. E. 1971 Vapor void fraction for forced convection with subcooled boiling at low flow rates. Ph.D. Thesis, Univ. of California, Berkeley; also, General Electric Company Rep. NEDO-10491, 1971.

WONG, S. & HOCHREITER, L. E. 1981 Analysis of the FLECHT-SEASET unblocked bundle steam cooling and boil-off tests. EPRI Report NP-1460.

IRELAND, J. K., MAST, P. K., WEHNER, T. R., BLEIWEIS, P. B., KIRCHNER, W. L. & STEVENSON, M. G.

1980 Preliminary calculation relation related to the accident at Three-Mile Island. NRC, NUREG, CR-1353 (LA8273-MS).

JONES, A. B. 1961 Hydrodynamic stability of a boiling channel. AEC Rep. KAPL 2170.

LELLOUCHE, G. L. & ZOLOTAR B. 1979 Private communication.

LARSON, T. K., LOOMIS, G. G. & SHUMWAY, R. W. 1979 Simulation of the Three-Mile Island transient in SEMISCALE. USNRC/EG&G Interim Rep. SEMI-TR-010.

NICKLIN, D. J., WILKES, J. O. DAVIDSON, J. F. 1962 Two-phase flow in vertical tubes. *Trans. Inst. Chem. Engrs.* **40**, 61.

NSAC 1979 Analysis of the Three-Mile Island-Unit 2 accident. Electric Power Research Institute Rep. NSAC-1; NSAC, 1980, Rep. NSAC-1 (revised).

SAHA, P. & ZUBER, N. 1974 Point of net vapor generation and vapor void fraction in subcooled boiling. Paper presented at the *5th Int. Heat Transfer Conf.*, Sept., Tokyo, Japan.

SEBAN, R. A. & KHARRAAZI, A. 1980 "Single tube reflood with subsequent boiling dry because of termination of feed. Electric Power Research Institute Rep. NP-80-4-LD.

SHUMWAY, R. W. 1979 Private communication.

VEA, H. W. & LAHEY, R. T. 1978 An exact analytical solution of pool swell dynamics during depressurization by the method of characteristics. *Nucl. Engng Design* **45**, 101–116.

WALLIS, G. B. 1969 *One-dimensional two-phase flow.* McGraw-Hill, New York.

WARD, L. W. 1979 Simplified small-break blowdown models. *Nucl. Tech.* **45**, 68–76.

WEDEKIND, G. L., BHATT, B. L. and BECK, B. T. 1978, "A system mean void fraction model for predicting various transient phenomena associated with two-phase evaporating and condensing flows," *Int. J. Multiphase Flow* **4**, 97–114.

WILSON, J. F., GRENDA, R. T. & PATTERSON, J. F. 1962 The velocity of rising steam in a bubbling two-phase mixture, *Trans. Am. Nucl. Soc.* **5**, 151–152.

ZUBER, N. & FINDLAY, J. A. 1965 Average volume concentration in two-phase flow systems, A.S.M.E. *J. of Heat Transfer* 453–468.

ZUBER, N. & STAUB, F. W. 1966 The propagation and wave form of the vapor volumetric concentration in boiling forced convection system under oscillatory conditions, *Int. J. Heat Mass Transfer* **9**, 871–895.

ZUBER, N. & STAUB, F. W. 1967 A analytical investigation of the transient response of the volumetric concentration in a boiling forced-flow system, *Nucl. Sci. Engng* **30**, 268–278.